

Precision Inflationary Predictions: Impact of Accurate End-of-Inflation Dynamics

Debottam Nandi^{1,*}, Simran Yadav^{2,†} and Manjeet Kaur^{2,‡}

¹*Department of Physics, School of Advanced Sciences,*

Vellore Institute of Technology (VIT) Chennai, Chennai 600127, India

²*Department of Physics and Astrophysics, University of Delhi, Delhi 110007, India*

The precision era of cosmology demands accurate theoretical predictions from inflationary models. In quantitative reheating analyses, inflationary observables depend sensitively on the number of e-folds between horizon exit and the end of inflation, N_k , whose determination relies on slow-roll approximations near the end of inflation. Since inflation ends when the first slow-roll parameter reaches unity, even modest inaccuracies in this approximation can shift the end of inflation and thereby alter N_k , leading to modifications in predicted observables—including those evaluated at leading-order. While such effects are implicit in standard treatments, their quantitative impact on observable constraints has not been systematically assessed. In this work, we first re-evaluate leading-order slow-roll predictions using an improved determination of N_k within a simple quantitative reheating framework, and then incorporate higher-order slow-roll corrections consistently with the revised background evolution. Applying this framework to the Starobinsky model, we find that improved end-of-inflation dynamics alone can induce shifts of order $\Delta n_s \sim 10^{-3}$, while higher-order slow-roll corrections provide additional refinements at the $\sim 4 \times 10^{-4}$ level. The cumulative effect yields a maximum shift of $\Delta n_s \sim 1.2 \times 10^{-3}$ within the allowed reheating range. To our knowledge, this is the first systematic decomposition of end-of-inflation corrections and their individual contributions to n_s in the Starobinsky model, with implications for model discrimination in next-generation CMB surveys. These results demonstrate that an accurate determination of the end of inflation is essential for precision tests of inflationary models.

Keywords: The Early Universe, Inflationary Paradigm, Reheating, CMB, Perturbations.

I. INTRODUCTION

The inflationary paradigm [1–31] provides a compelling description of the early universe, resolving the horizon and flatness problems while generating primordial perturbations in excellent agreement with observations of the cosmic microwave background and large-scale structure. In

* debottam.nandi@vit.ac.in

† simranyadavkhola@gmail.com

‡ mkaur1@physics.du.ac.in

particular, slow-roll inflationary models predict an almost scale-invariant spectrum of fluctuations consistent with current data [32–35]. As cosmological observations steadily improve in precision, however, the reliability of inflationary predictions increasingly depends on the accuracy of the underlying theoretical framework. In this precision-driven context, effects that are traditionally regarded as subleading can become observationally relevant, motivating a reassessment of standard approximation schemes.

Connecting inflationary predictions to observations requires accounting for the post-inflationary evolution of the universe, in particular the reheating epoch that bridges inflation and the radiation-dominated era [36–58]. In quantitative analyses [44, 45, 47, 49, 52, 54, 59–64], reheating is commonly characterized by an effective equation-of-state parameter and the duration of the reheating phase, which together determine the number of e-folds between horizon exit of observable modes and the end of inflation. Since inflationary observables, such as the scalar spectral index n_s and the tensor-to-scalar ratio r , are highly sensitive to this duration, uncertainties in reheating directly propagate into predicted cosmological parameters.

Despite the sensitivity of inflationary predictions to post-inflationary evolution, it is commonly assumed that leading-order slow-roll approximations provide sufficiently accurate estimates of the inflationary background dynamics, including the determination of the end of inflation. In standard treatments, the end of inflation is inferred from slow-roll conditions, although inflation strictly terminates when the first slow-roll parameter reaches unity. Even modest inaccuracies in this approximation shift the end of inflation and therefore modify the duration of inflation. Since the number of e-folds N_k between horizon exit and the end of inflation depends directly on this endpoint, a careful and consistent determination of the end of inflation becomes essential for reliable theoretical predictions.

The central role of N_k becomes particularly evident in quantitative reheating analyses, where it appears explicitly in the consistency relation that connects the comoving pivot scale to the post-inflationary expansion history. More precisely, N_k depends on both the effective reheating equation-of-state parameter w_{re} and the reheating duration N_{re} , subject to the physical constraint $N_{\text{re}} \geq 0$, where $N_{\text{re}} \ll 1$ corresponds to instantaneous reheating. Through this relation, N_k determines the value of the inflaton field at horizon exit and hence the slow-roll parameters that enter predictions for observables such as the scalar spectral index n_s and the tensor-to-scalar ratio r . Even within leading-order slow-roll expressions, small shifts in N_k directly translate into corrections to n_s and r at a level comparable to current [32–35] and forthcoming observations such as PRISM [65], EUCLID [66], cosmic 21-cm surveys [67], and CORE [68] sensitivities. As cosmo-

logical measurements continue to improve in precision, achieving reliable theoretical control over the determination of N_k becomes increasingly important. Moreover, inflationary predictions and their post-inflationary reheating constraints have been explored across a wide variety of theoretical frameworks, including warm inflation with Chaplygin gas backgrounds [69, 70], warm tachyon scalar field inflation [71], warm inflation in $f(\phi, T)$ modified gravity [72], and attractor models in extended teleparallel gravity [73] — all of which confirm that precise control of inflationary observables and their post-inflationary history is essential for consistency with CMB data. However, in most standard treatments, the effect of accurately determining the end of inflation is implicitly assumed to be negligible and has not been systematically quantified.

Motivated by this sensitivity, the primary objective of this work is to obtain a more reliable determination of the duration of inflation and the corresponding number of e-folds N_k by improving the treatment of the inflationary background dynamics near the end of inflation. Since inflation terminates when the first slow-roll parameter reaches unity, even modest inaccuracies in the slow-roll approximation can shift the end of inflation and thereby alter N_k , leading to modifications in inflationary observables — including those evaluated at leading-order. While recent studies [74, 75] have indicated that improved treatments of the background evolution can induce non-negligible corrections to the estimation of N_k , these effects have not been systematically quantified with explicit numerical implications for inflationary observables — nor has the individual contribution of each correction been isolated and decomposed separately. In this work, we address this gap by carrying out a detailed analysis in two stages. First, we reassess leading-order slow-roll predictions using an improved determination of N_k within a simple and controlled quantitative reheating framework, thereby isolating the impact of end-of-inflation corrections on baseline theoretical predictions. Second, we incorporate higher-order slow-roll corrections [76–90] consistently with the revised background evolution to evaluate additional refinements. As a representative and observationally viable benchmark, we apply this framework to the Starobinsky model of inflation [1, 2, 8, 91, 92] and demonstrate that corrections often regarded as negligible can lead to appreciable modifications of inflationary predictions — specifically, a cumulative shift of $\Delta n_s \sim 1.2 \times 10^{-3}$ in the scalar spectral index, dominated by the numerical background treatment ($\sim 10^{-3}$), with subdominant contributions from higher-order slow-roll terms ($\sim 4 \times 10^{-4}$) and the revised reheating onset ($\sim 10^{-5}$). To our knowledge, this is the first systematic decomposition of these corrections and their individual propagation into n_s for the Starobinsky model, with direct implications for model discrimination in next-generation CMB surveys operating at sensitivity $\Delta n_s \sim 10^{-3}$.

This article is organized as follows. In Sec. II, we introduce the inflationary model and the

corresponding background dynamics, including the slow-roll conditions and the associated approximations. Sec. III presents the quantitative reheating analysis that connects inflationary perturbations to observable constraints, where the Starobinsky model is examined as a representative example using leading-order slow-roll expressions. In Sec. IV, we implement corrections to the inflationary dynamics and assess their impact on theoretical predictions and reheating constraints. Our conclusions are summarized in Sec. V.

Throughout this work, we employ natural units with $\hbar = c = k_B = 1$ and set the reduced Planck mass to $M_{\text{pl}} \equiv (8\pi G)^{-1/2} = 1$. The metric signature is $(-, +, +, +)$, Greek indices are contracted with the spacetime metric $g_{\mu\nu}$, and Latin indices with the Kronecker delta δ_{ij} . We denote partial and covariant derivatives by ∂ and ∇ , respectively, while overdots and primes represent derivatives with respect to cosmic and conformal time in the Friedmann–Lemaître–Robertson–Walker background.

II. GENERAL EQUATIONS AND SLOW-ROLL CONDITIONS

In this section, we present the general background equations governing single-field inflation and review the standard slow-roll framework that underlies conventional analytical predictions. This formulation will serve as the baseline against which we later assess corrections arising from a more accurate treatment of the end of inflation. For that, let us consider the simplest action with a single canonical scalar field ϕ minimally coupled to gravity with a potential $V(\phi)$, which can be written as

$$S = \frac{1}{2} \int d^4x \sqrt{-g} [R - g^{\mu\nu} \partial_\mu \phi \partial_\nu \phi - 2V(\phi)]. \quad (1)$$

Here, R is the Ricci scalar. The corresponding equations of motion, i.e., Einstein's equations and the equation of the scalar field, can be written as

$$R_{\mu\nu} - \frac{1}{2} g_{\mu\nu} R = T_{\mu\nu(\phi)}, \quad (2)$$

$$\nabla_\mu T^{\mu\nu}_{(\phi)} = 0, \quad (3)$$

where $T^{\mu}_{\nu(\phi)}$ is the stress-energy tensor corresponding to the ϕ field and can be written as

$$T_{\mu\nu(\phi)} = \partial_\mu \phi \partial_\nu \phi - g_{\mu\nu} \left(\frac{1}{2} \partial_\lambda \phi \partial^\lambda \phi + V(\phi) \right). \quad (4)$$

Using the flat FLRW line element describing the homogeneous and isotropic universe at large scales, i.e.,

$$ds^2 = -dt^2 + a^2(t) d\mathbf{x}^2, \quad (5)$$

where, $a(t)$ is the scale factor, Eqs. (2) and (3) can be reduced to

$$3H^2 = \frac{1}{2}\dot{\phi}^2 + V(\phi), \quad (6)$$

$$\dot{H} = -\frac{1}{2}\dot{\phi}^2, \quad (7)$$

$$\ddot{\phi} + 3H\dot{\phi} + V_{,\phi} = 0. \quad (8)$$

where, $H \equiv \dot{a}/a$ is the Hubble parameter, and $A_x \equiv \partial A/\partial x$. These equations can be re-defined in terms of the e-fold variable $N \equiv \int H dt = \ln(a/a_0)$ as

$$H^2 = \frac{V}{3 - \frac{1}{2}\phi_N^2}, \quad \frac{H_N}{H} = -\frac{1}{2}\phi_N^2, \quad (9)$$

$$\phi_{NN} + \left(3 - \frac{1}{2}\phi_N^2\right) \left(\phi_N + \frac{V_{,\phi}}{V}\right) = 0, \quad (10)$$

where, $A_{xx} = \partial^2 A/\partial x^2$. For a given potential $V(\phi)$, these equations fully determine the background dynamics of inflation. In conventional analyses, these equations are typically simplified under the slow-roll approximation, yielding analytical expressions for inflationary observables. In the following, we briefly review this standard framework, which will serve as the baseline for the improved treatment developed later in this work.

Once the background equations are solved, one can in principle solve the scalar (\mathcal{R}_k) and tensor (h_k) perturbations and evaluate the power spectra:

$$\mathcal{P}_{\mathcal{R}} = \frac{k^3}{2\pi^2} |\mathcal{R}_k|^2 \equiv A_{\mathcal{R}} \left(\frac{k}{k_*}\right)^{n_s-1}, \quad \mathcal{P}_T = 2 \cdot \frac{k^3}{2\pi^2} |h_k|^2 \equiv A_T \left(\frac{k}{k_*}\right)^{n_T} \quad (11)$$

where, k_* is the pivot scale, $A_{\mathcal{R}}$, A_T are the scalar and tensor spectral amplitude,

$$n_s \equiv \left. \frac{d \ln \mathcal{P}_{\mathcal{R}}}{d \ln k} \right|_{k=k_*}, \quad n_T \equiv \left. \frac{d \ln \mathcal{P}_T}{d \ln k} \right|_{k=k_*}$$

are the scalar and tensor spectral indices and

$$r \equiv \frac{A_T}{A_{\mathcal{R}}}$$

is defined as the tensor-to-scalar ratio. The current observations constrain $A_{\mathcal{R}} \simeq 2.101_{-0.034}^{+0.031} \times 10^{-9}$ (68% CL), $n_s = 0.9672 \pm 0.0059$ (68% CL) and $r < 0.028$ (95% CL) at $k_* = 0.05 \text{ Mpc}^{-1}$ (PLANCK [32, 33, 35], BICEP/Keck [34]). These observations agree remarkably well with the predictions of a near-scale-invariant spectrum of density perturbations in the inflationary paradigm. In the next section, we will discuss in detail how, without explicitly evaluating the perturbations, one can obtain these observables using the background solutions in the case of slow-roll inflation.

Slow-roll inflation

We adopt the Hubble-flow definition of slow-roll parameters. Let us first define the two slow-roll parameters ϵ_1 and ϵ_2 as

$$\epsilon_1 \equiv -\frac{\dot{H}}{H^2} = \frac{1}{2}\dot{\phi}_N^2, \quad \epsilon_2 \equiv \frac{\dot{\epsilon}_1}{H\epsilon_1} = 2\frac{\phi_{NN}}{\phi_N}. \quad (12)$$

While $\epsilon_1 < 1$ ensures that the universe is accelerating, the condition $\epsilon_2 \ll 1$ ensures the sufficient duration of the inflationary phase. Inflation ends when the first slow-roll parameter reaches unity, i.e., $\epsilon_1 = 1$, without invoking slow-roll approximations. In the case of slow-roll, both these parameters are extremely small, i.e.,

$$\epsilon_1 \ll 1, \quad \epsilon_2 \ll 1. \quad (13)$$

These two conditions are also referred to as the slow-roll conditions. Under these conditions, Eqs. (9) and (10) become

$$H^2 \simeq \frac{1}{3}V, \quad \phi_N \simeq -\frac{V_\phi}{V}, \quad (14)$$

and, using the above equation, the slow-roll parameters can be re-expressed in terms of shape of potential as

$$\epsilon_1 \simeq \frac{1}{2} \left(\frac{V_\phi}{V} \right)^2, \quad \epsilon_2 \simeq 2 \left(\frac{V_\phi^2}{V^2} - \frac{V_{\phi\phi}}{V} \right). \quad (15)$$

Eqs. (14) are referred to as the slow-roll equations. By solving these simplified equations, one can obtain the approximate analytical solution of the Hubble parameter as well as the slow-roll parameters, and thus the dynamics of the universe in slow-roll regime.

In order to check for consistency with the observation, one can, in principle, obtain the observables corresponding to the perturbations associated with the pivot scale k in terms of slow-roll parameters as

$$A_{\mathcal{R}} \simeq \frac{H^2}{8\pi^2\epsilon_1}, \quad n_s \simeq 1 - 2\epsilon_1 - \epsilon_2, \quad r \simeq 16\epsilon_1. \quad (16)$$

The above expressions are obtained using leading-order slow-roll approximation, assuming the higher-order contributions are heavily suppressed. These observables depend explicitly on the e-folding number N_k , defined as the interval between horizon exit of the pivot scale and the end of inflation. Since N_k is determined by the precise end of inflation, any inaccuracy in the slow-roll estimation of the end-of-inflation propagates directly into these leading-order predictions. Typically,

this duration is considered to be $N_k \sim 50 - 60$. However, as we shall demonstrate, even shifts of order unity in N_k can translate into corrections in n_s at the level of 10^{-3} , which is comparable to present and projected observational precision. However, it is a model-dependent quantity and in order to obtain the exact duration N_k , one must consider the post-inflationary dynamics, i.e., the reheating epoch. A consistent determination of N_k therefore requires incorporating the post-inflationary expansion history. In the next section, we implement this through the quantitative analysis of reheating.

III. QUANTITATIVE ANALYSIS OF REHEATING

As mentioned in the previous section, in the slow-roll regime, the slow-roll parameters are very small, i.e., $\epsilon_1, \epsilon_2 \ll 1$. However, as the field rolls down the potential, these slow-roll parameters increase, and the inflation ends as soon as this condition is violated, i.e., $\epsilon_1 = 1$. Briefly, after the end of inflation, the field reaches the bottom and begins to oscillate around it and couples with the other (standard) particles. As a consequence, at this stage, the time average of kinetic energy is the same as the average of the potential energy, and the field decays. This epoch is known as the reheating phase.¹

This epoch involves intricate microphysical processes and is largely model-dependent. As a result, any analytical extension of its dynamics carries substantial uncertainties, making it extremely challenging to describe the epoch through a single, unified analytical framework. To circumvent this difficulty and achieve a model-independent treatment, a simplified quantitative approach has been developed in which the equation-of-state parameter during the entire reheating epoch, i.e., w_{re} is assumed to remain constant. Although this approximation does not capture the full microphysical complexity of reheating, it provides a useful average macrophysical description that successfully connects inflationary predictions with observations and thereby enables broad, indirect constraints on the reheating scenario. In this case, the energy density during reheating effectively behaves as

$$\rho \propto a^{-3(1+w_{\text{re}})}. \quad (17)$$

This relation follows from energy conservation $\dot{\rho} + 3H(1+w)\rho = 0$. We also define the duration of

¹ It is worth noting that in warm inflationary scenarios [69–73, 93–97], the inflaton continuously transfers energy to a thermal radiation bath *during* inflation itself, so the distinct post-inflationary reheating phase analyzed here does not apply; the present work focuses exclusively on standard cold inflation followed by a separate reheating era, characterized by an effective equation-of-state parameter w_{re} and duration N_{re} . A study of how end-of-inflation dynamics interplay with dissipation in warm scenarios is left to future work.

reheating N_{re} as

$$N_{\text{re}} \equiv \ln \left(\frac{a_{\text{re}}}{a_{\text{end}}} \right) \quad (18)$$

where a_{end} , a_{re} are the scale factor solutions at the end of the inflation and reheating epoch, respectively. Physical consistency requires $N_{\text{re}} \geq 0$, where $N_{\text{re}} \ll 1$ corresponds to instantaneous reheating. In order to calculate the duration N_{re} , let us compare the mode of interest with the present scale as

$$\frac{k}{a_0 H_0} = \frac{a_k H_k}{a_0 H_0} = \frac{a_k}{a_{\text{end}}} \frac{a_{\text{end}}}{a_{\text{re}}} \frac{a_{\text{re}}}{a_{\text{eq}}} \frac{a_{\text{eq}}}{a_0} \frac{H_k}{H_{\text{eq}}} \frac{H_{\text{eq}}}{H_0}, \quad (19)$$

where k is the comoving scale, and (eq) and (0) denote the quantities at the matter-radiation equality and the present epoch, respectively. Then the above equation leads to:

$$\ln \left(\frac{k}{a_0 H_0} \right) = -N_k - N_{\text{re}} - N_{\text{RD}} + \ln \left(\frac{a_{\text{eq}} H_{\text{eq}}}{a_0 H_0} \right) + \ln \left(\frac{H_k}{H_{\text{eq}}} \right), \quad (20)$$

where $N_k \equiv \ln \left(\frac{a_{\text{end}}}{a_k} \right)$, $N_{\text{RD}} \equiv \ln \left(\frac{a_{\text{eq}}}{a_{\text{re}}} \right)$. At the end of reheating, the energy density is

$$\rho_{\text{re}} = \frac{\pi^2}{30} g_{\text{re}} T_{\text{re}}^4, \quad (21)$$

where, g_{re} is the effective number of relativistic species upon thermalization. Radiation drives the ensuing expansion, with non-relativistic matter and dark energy making recent additions. Assuming a negligible entropy shift following T_{re} , the current CMB and neutrino background both retain the reheating entropy, which leads to the relation,

$$g_{\text{s, re}} T_{\text{re}}^3 = \left(\frac{a_0}{a_{\text{re}}} \right)^3 \left(2T_0^3 + 6 \times \frac{7}{8} T_{\nu 0}^3 \right), \quad (22)$$

where the present (CMB) temperature, $T_0 \simeq 2.73$ K, the neutrino temperature, $T_{\nu 0} = (4/11)^{1/3} T_0$, and $g_{\text{s, re}}$ is the effective number of species for entropy at reheating. Therefore, T_{re} can be written as the present temperature T_0 as

$$\frac{T_{\text{re}}}{T_0} = \frac{a_0}{a_{\text{eq}}} \frac{a_{\text{eq}}}{a_{\text{re}}} \left(\frac{43}{11g_{\text{s, re}}} \right)^{1/3}, \quad (23)$$

and the Eq. (20) can be re-written as

$$N_{\text{re}} = \frac{4}{1 - 3w_{\text{re}}} \left[-N_k - \frac{1}{4} \ln \left(\frac{30}{\pi^2 g_{\text{re}}} \right) - \frac{1}{3} \ln \left(\frac{11g_{\text{s, re}}}{43} \right) - \ln \left(\frac{k}{a_0 T_0} \right) - \frac{1}{4} \ln \left(\frac{\rho_{\text{end}}}{H_k^4} \right) \right]. \quad (24)$$

and T_{re} can be reduced to the following form:

$$T_{\text{re}} = \frac{a_0 T_0}{k} \left(\frac{43}{11g_{\text{s, re}}} \right)^{1/3} H_k e^{-N_k - N_{\text{re}}}. \quad (25)$$

where H_k can be written as

$$H_k = \pi \sqrt{\frac{r A_{\mathcal{R}}}{2}}. \quad (26)$$

Please note that the Hubble parameter H_k is a function of duration N_k , and therefore, N_{re} is eventually a function of N_k . As spectral index n_s (or any time-dependent parameters like the field ϕ or tensor-to-scalar ratio r) depends on N_k , considering $\{g_{\text{re}}, g_{\text{s, re}}\} \sim 100$, one can plot n_s vs. N_{re} (or T_{re} from the above expression) and obtain a strict constraint on N_{re} [25, 47, 53, 55, 59, 98, 99] as n_s is strictly bounded. This is referred to as the quantitative analysis of reheating. In the next section, we will elaborately discuss this analysis by implementing it on the Starobinsky model of inflation.

A. Starobinsky inflation

One of the most successful models of slow-roll inflation is the Starobinsky model [1, 2, 8, 91, 92] where the potential in the Einstein frame is given by:

$$V(\phi) = \frac{3}{4} M^2 \left(1 - e^{-\sqrt{2/3}\phi}\right)^2, \quad (27)$$

where M is the mass of the scalar field ϕ , whose value is constrained by the normalization of the scalar power spectrum to the CMB amplitude $\mathcal{A}_{\mathcal{R}} \simeq 2.1 \times 10^{-9}$, yielding $M \approx 1.3 \times 10^{-5} M_{\text{pl}}$. As-

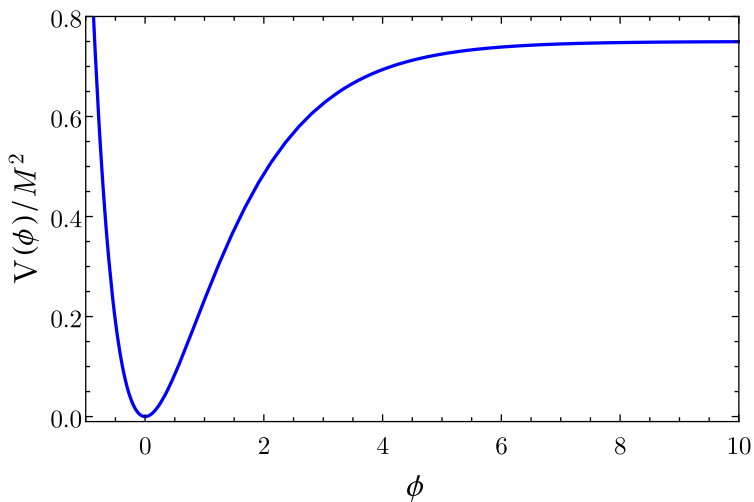


FIG. 1. The Starobinsky potential given in Eq. (27).

suming the slow-roll conditions are satisfied, we can immediately obtain the two slow-roll equations (i.e., Eqs. (14)) as

$$H \simeq \frac{M}{2} \left(1 - e^{-\sqrt{2/3}\phi}\right), \quad \phi_N \simeq -2\sqrt{\frac{2}{3}} \frac{e^{-\sqrt{2/3}\phi}}{\left(1 - e^{-\sqrt{2/3}\phi}\right)}, \quad (28)$$

and the slow-roll parameters can be expressed in terms of the field ϕ as (i.e., Eqs. (15)):

$$\epsilon_1 \simeq \frac{4e^{-2\sqrt{2/3}\phi}}{3\left(1 - e^{-\sqrt{2/3}\phi}\right)^2}, \quad \epsilon_2 \simeq \frac{8e^{-\sqrt{2/3}\phi}}{3\left(1 - e^{-\sqrt{2/3}\phi}\right)^2}. \quad (29)$$

With the help of Eq. (28), one can easily solve the scalar field solution in terms of the e-folding number N_k , and the solutions of the slow-roll parameters at the leading-order, for $N_k \gg 1$, can be obtained as:

$$\epsilon_1 \simeq \frac{3}{4N_k^2}, \quad \epsilon_2 \simeq \frac{2}{N_k}, \quad (30)$$

and, using the leading-order slow-roll approximation, i.e., Eqs. (16), we can quickly evaluate the scalar spectral index and the tensor-to-scalar ratio in terms of the e-folding number as:

$$n_s \simeq 1 - \frac{2}{N_k}, \quad r \simeq \frac{12}{N_k^2}. \quad (31)$$

Using the above equation along with Eqs. (24) and (25), one can obtain parametric dependence of N_{re} and T_{re} on n_s . In the case of the Starobinsky model, this is shown in Fig. 2. Keep in mind that, $N_{\text{re}} \geq 0$, with $N_{\text{re}} \ll 1$ is referred to as instantaneous reheating [99, 100]. It immediately leads to the constraint on the value of n_s . For example, considering that during reheating, the evolution of the universe effectively behaves as matter-expansion, i.e., $w_{\text{re}} = 0$. Thus, in the 1σ domain, we get the bound on N_k as

$$52 \leq N_k \leq 56 \quad (32)$$

for $w_{\text{re}} = 0$, and correspondingly, the bound on n_s becomes:

$$0.961 \leq n_s \leq 0.964. \quad (33)$$

These bounds follow from imposing the observational constraint on n_s together with the physical requirement $N_{\text{re}} \geq 0$. In fact, as can be seen, for $w_{\text{re}} < 1/3$, it is obvious that there is an upper bound on N_k , which implies a bound on n_s as well, i.e., $N_k \leq 56$ and $n_s < 0.964$. It also immediately puts a tight constraint on N_{re} and T_{re} (for $w_{\text{re}} = 0$) as

$$N_{\text{re}} \leq 16, \quad T_{\text{re}} \geq 10^{10} \text{ GeV}. \quad (34)$$

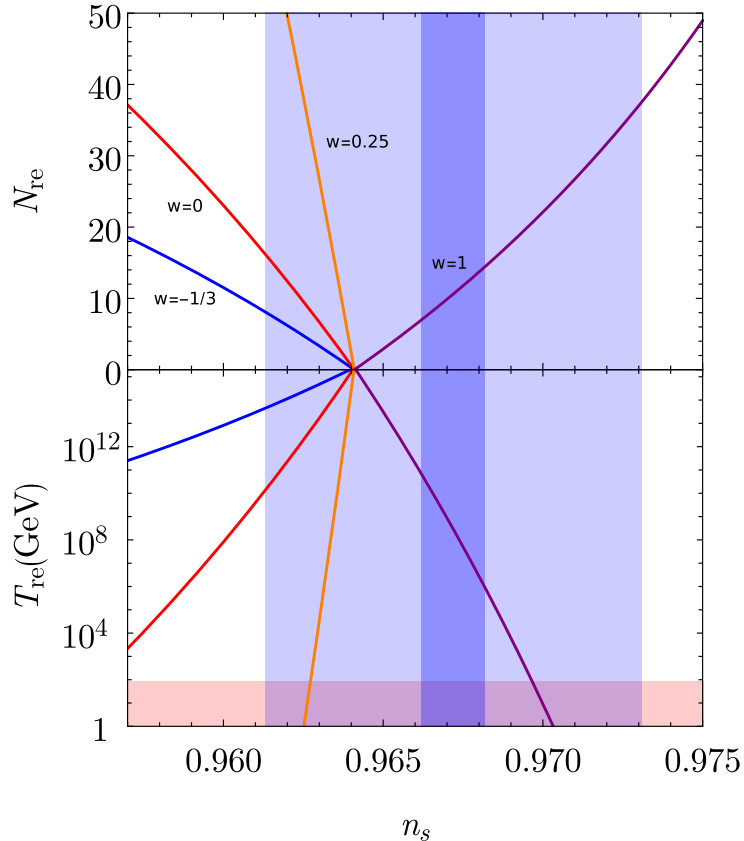


FIG. 2. We plot the duration of reheating N_{re} and reheating temperature T_{re} given in Eqs. (24) and (25) as functions of the scalar spectral index n_s given by Eq. (31) using leading-order slow-roll approximations for the case of Starobinsky inflation. Please note that different colors represent dynamics corresponding to different effective EoS parameter w_{re} as indicated in the figure. The blue-shaded region represents the 1σ constraint on the value of n_s using ongoing observations [32–35] with $n_s = 0.9672 \pm 0.0059$. The dark blue region shows the future projected bound on n_s with a sensitivity of 10^{-3} , assuming its central value remains unchanged. The temperature below the lighter red region is excluded due to the constraint from the electroweak scale, which is taken to be 100 GeV.

However, during reheating, if we assume $w_{\text{re}} > 1/3$, these constraints flip and in the 1σ domain, there arises a new bound with a lower value of N_k as well as in n_s as

$$56 \leq N_k \leq 74, \quad 0.964 \leq n_s \leq 0.973. \quad (35)$$

Consequently, the bound on reheating parameters becomes (for $w_{\text{re}} = 1$)

$$N_{\text{re}} \leq 37, \quad T_{\text{re}} \geq 10^{-9} \text{ GeV}. \quad (36)$$

Note that reheating temperatures below the BBN scale (~ 10 MeV) are observationally excluded; therefore, the region corresponding to $T_{\text{re}} \leq 10^{-2}$ GeV is not physically viable and must be dis-

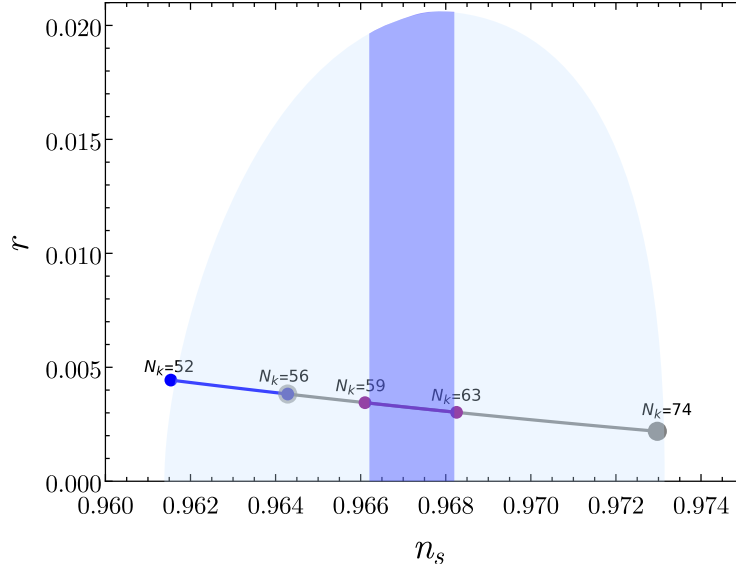


FIG. 3. We plot the inflationary observables, tensor-to-scalar ratio (r) as a function of scalar spectral index (n_s) for the Starobinsky model using leading-order slow-roll approximations given by Eq. (31). This evolution is presented considering the bound on duration N_k using the reheating regime. We consider different EoS parameters during reheating w_{re} and observe the constraint on the duration N_k . Correspondingly, in the figure, blue line corresponds to the bound for $w_{\text{re}} < 1/3$, the gray line for $w_{\text{re}} > 1/3$ and the purple line for the future observational bound of n_s . The blue-shaded region represents the 1σ constraint on the value of n_s using ongoing observations [32–35] with $n_s = 0.9672 \pm 0.0059$. The dark blue region shows the future projected bound on n_s with a sensitivity of 10^{-3} , assuming its central value remains unchanged.

carded. In addition, considerations related to the electroweak scale (~ 100 GeV) may motivate a higher reheating temperature in specific baryogenesis scenarios; however, this requirement is model-dependent and does not provide a constraint as robust as the BBN bound. Taking these bounds into account, we plot r as a function of n_s in Fig. 3. Further, instead of looking in 1σ limit, if we consider the observational constraints proposed by the forthcoming experiments such as PRISM [65], EUCLID [66], cosmic 21-cm surveys [67], and CORE [68] experiments, which offer a precision enhancement of 10^{-3} in n_s , the constraints on N_k , N_{re} and T_{re} can be substantially improved². Then one can immediately refer from the Fig. 2 and 3 that for $w_{\text{re}} < 1/3$, the scalar spectral index does not satisfy the constraints in 1σ level posed by future observations. Therefore, under these conditions, this model would be disfavored at the 1σ level if the central value remains unchanged. The model can survive if one assumes $w_{\text{re}} > 1/3$, and the bound on N_{re} and T_{re} for

² The central value of n_s is assumed to be 0.9672 [35]

the constraints posed by future observations becomes

$$7 \leq N_{\text{re}} \leq 14, \quad 10^9 \text{ GeV} \geq T_{\text{re}} \geq 10^6 \text{ GeV}. \quad (37)$$

Even in that case, if the future observations detect instantaneous reheating [99, 100], i.e., $N_{\text{re}} \ll 1$, n_s appears to be outside of the contour from the future observations. Therefore, unless $w > 1/3$ with the prolonged reheating era, the analytical approximation may lead to ruling out the Starobinsky inflation model. However, keeping aside the future observations, in the next section, we will see a significant improvement in these constraints by implementing meaningful corrections to the dynamics rather than the analytical approximations.

IV. NUMERICAL IMPROVEMENTS

In the previous section, we discussed the CMB constraints on various inflationary models, which depend on the effective EoS parameter w_{re} as well as the duration of the reheating epoch N_{re} . There are two issues associated with this analysis. First, around and at the end of inflation, the slow-roll approximation breaks down. Yet, in evaluating duration N_k as well as energy density at end of inflation ρ_{end} in Eq. (24), we rely upon slow-roll approximations. Second, in evaluating perturbed observables in Eqs. (16), we consider only the leading-order contributions and ignore higher-order contributions, assuming their impact to be negligible. However, as anticipated in Refs. [74, 75], considering accurate dynamics rather than the slow-roll approximations may lead to notable enhancements in these predictions. Additionally, one can consider the onset of reheating not at the end of inflation but at the bottom of the potential, as will be discussed in the subsequent section. The implementation and, therefore, the resulting corrections due to these considerations can be categorized into three parts:

1. Implementation of accurate inflationary dynamics through numerical methods instead of slow-roll approximations.
2. Implementation of higher-order slow-roll approximations instead of leading-order slow-roll approximations.
3. Implementation of onset of reheating as the bottom of the potential instead of the end of inflation.

In the following sections, we will conduct a detailed study of the impact of each of these corrections

on the observational constraints. We will also compare the cumulative effects of these corrections with the existing predictions presented in the previous section.

A. Implementation of accurate inflationary dynamics through numerical methods

As mentioned earlier, this epoch of the slow-roll regime lasts as long as both of the slow-roll parameters are small, i.e., ($\epsilon_1 \ll 1$, $\epsilon_2 \ll 1$). On the other hand, $\epsilon_1 = 1$ signals the end of inflation. It turns out that even before the end of inflation, these slow-roll approximations break down. Despite this, we still rely on (leading-order) slow-roll approximations even at the end of inflation to determine the analytical solution of the background variables, assuming the contribution due to accurate dynamics in evaluating perturbed observables is negligible. While slow-roll remains an excellent approximation during most of the inflationary phase, its validity deteriorates near the end of inflation where $\epsilon_1 \rightarrow 1$, and the higher-order kinetic contributions become non-negligible. However, it is crucial, as in this section, we shall learn the significance of obtaining the accurate values of not only the background parameters but also the end of inflation. To illustrate this, let's now discuss this in detail with an example: the Starobinsky inflation.

Using leading-order slow-roll approximations and solving the slow-roll equations (*viz.* Eqs. (14)):

$$H^2 \simeq \frac{V}{3}, \quad \phi_N \simeq -\frac{V_\phi}{V},$$

with the initial condition $\phi_i = 5.8$, we obtain the following results:

$$N_{\text{end}} \simeq 80.86, \quad \phi_{\text{end}} \simeq 0.94, \quad H_{\text{end}} \simeq 0.267 M, \quad \rho_{\text{end}} \simeq 0.215 M^2,$$

along with the slow-roll solutions given in Eqs. (30). In both the analytical and numerical cases, we impose the identical initial condition $\phi_i = 5.8$ to ensure a consistent comparison. Here, N_{end} is the duration of the field rolling from the initial value ϕ_i to ϕ_{end} , i.e., the duration of inflation. These values are essential for the analysis in Eqs. (24) and (25) which has been shown in the previous section with Fig. 2.

To improve the analysis, in this section, we now consider, rather than the slow-roll, the full inflationary equations (*viz.* Eqs. (9) and (10)):

$$H = \sqrt{\frac{V}{3 - \frac{1}{2}\phi_N^2}}, \quad \phi_{NN} + \left(3 - \frac{1}{2}\phi_N^2\right) \left(\phi_N + \frac{V_\phi}{V}\right) = 0.$$

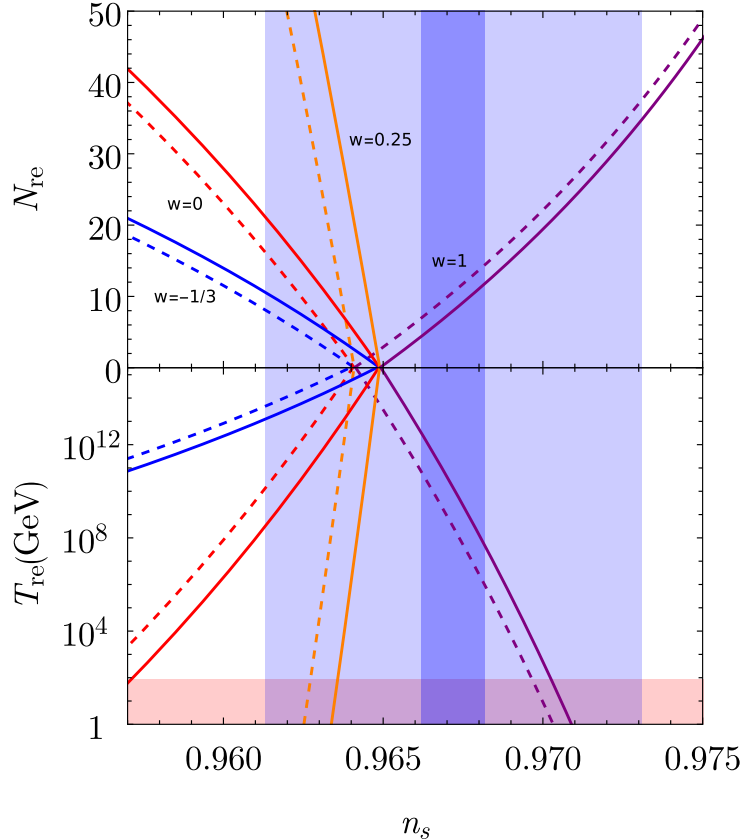


FIG. 4. We plot the duration of reheating N_{re} and reheating temperature T_{re} given by Eqs. (24) and (25) as functions of the scalar spectral index n_s parametrically for both analytical and numerical solution, given by Eqs. (31) and (16), respectively. The solid lines are for the numerical solution, and the dashed lines are for the analytically approximated solution. Please note that different colors represent dynamics corresponding to different effective equations of state parameter w_{re} as indicated in the figure. The blue-shaded region represents the 1σ constraint on the value of n_s using ongoing observations [32–35] with $n_s = 0.9672 \pm 0.0059$. The dark blue region shows the future projected bound on n_s with a sensitivity of 10^{-3} , assuming its central value remains unchanged. The temperature below the lighter red region is excluded due to the constraint from the electroweak scale, which is taken to be 100 GeV.

Solving the highly non-linear differential equation with identical initial condition $\phi_i = 5.8$ by using fourth-order Runge-Kutta (RK4) with adaptive step-size control, we now obtain the numerical solutions of the background variables such as the Hubble parameter and the slow-roll parameters along with:

$$N_{\text{end}} \simeq 82.48, \quad \phi_{\text{end}} \simeq 0.61, \quad H_{\text{end}} = 0.241 M, \quad \rho_{\text{end}} \simeq 0.175 M^2.$$

Thus, the numerical treatment shifts the end of inflation by $\Delta N_{\text{end}} \simeq 1.6$, which directly prop-

agates into the reheating analysis. These improvements directly impact the reheating analysis in two ways. The first is the direct influence of ρ_{end} in Eq. (24). The second, and more crucial, impact is the significant improvement in $\Delta N_{\text{end}} = \Delta N_k \sim 1.5$, which in turn enhances the accuracy of the background variables. For example, in the case of leading-order approximations, $\{\epsilon_1, \epsilon_2\} \simeq \{0.0003, 0.040\}$ for $N_k = 50$, whereas, numerically we obtain these values as $\{\epsilon_1, \epsilon_2\} \simeq \{0.00027, 0.038\}$, leading to a representative shift of $\Delta n_s \simeq 2 \times 10^{-3}$ around $N_k \simeq 50$, as also discussed in Ref. [74]³.

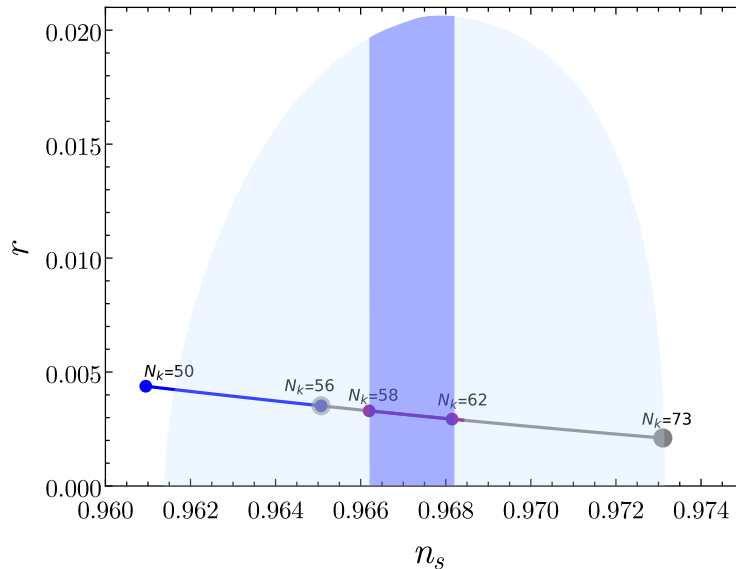


FIG. 5. We plot the inflationary observables, tensor-to-scalar ratio (r) as a function of scalar spectral index (n_s) for the Starobinsky model using numerical solution given by Eq. (16). This evolution is presented considering the bound on duration N_k using the reheating regime. We consider different EoS parameters during reheating w_{re} and observe the constraint on the duration N_k . Correspondingly, in the figure, blue line corresponds to the bound for $w_{\text{re}} < 1/3$, the gray line for $w_{\text{re}} > 1/3$ and the purple line for the future observational bound of n_s . The blue-shaded region represents the 1σ constraint on the value of n_s using ongoing observations [32–35] with $n_s = 0.9672 \pm 0.0059$. The dark blue region shows the future projected bound on n_s with a sensitivity of 10^{-3} , assuming its central value remains unchanged.

We now examine the impact of this on the reheating analysis and compare them with those obtained using slow-roll approximations. This is illustrated in Fig. 4. As anticipated, the improvement is significant. In the figure, one can see that numerical predictions show a significant shift to the right in the estimates of N_{re} and T_{re} . Due to this shift, the bound on N_k , and subsequently n_s

³ Please note that, for a multi-parameter model, numerical evaluation for the entire range of the parameters can be challenging. In that case, one can rely upon a semi-analytical solution presented in Ref. [74], where analytically obtained solutions are nearly comparable to the numerical solutions.

also changes, with an improvement being $\Delta n_s \sim 10^{-3}$. For example, in the case of leading-order slow-roll approximation with $w_{\text{re}} < 1/3$, the upper bound on n_s is: $n_s \leq 0.964$, whereas, in this improved case, the bound becomes $n_s \leq 0.965$. The improvements are explicitly shown in Table I. This confirms our anticipation that the accurate dynamics help improve the theoretical predictions, which is one of the main results of this work.

The physical origin of this correction deserves emphasis. In the slow-roll approximation, the end of inflation is defined by $\epsilon_1^{\text{sr}} = 1$, where $\epsilon_1^{\text{sr}} \equiv (V_{,\phi}/V)^2/2$ is computed purely from the potential. However, as inflation approaches its end, the kinetic energy of the inflaton $\frac{1}{2}\dot{\phi}^2$ becomes a non-negligible fraction of the total energy density $\rho = \frac{1}{2}\dot{\phi}^2 + V(\phi)$, and the Friedmann equation can no longer be approximated as $3H^2 \simeq V(\phi)$. Consequently, the slow-roll approximation *underestimates* the kinetic contribution near $\epsilon_1 \rightarrow 1$, causing the analytical treatment to misidentify the true end of inflation. This leads to a systematic overestimate of ρ_{end} and an underestimate of N_{end} , which in turn biases N_k and shifts n_s at the level of $\Delta n_s \sim 10^{-3}$. The full numerical integration of Eqs. (9) and (10) resolves this by tracking the exact phase-space trajectory of $(\phi, \dot{\phi})$ without invoking the slow-roll hierarchy, and thus correctly captures the moment $\epsilon_1 = 1$ is reached. For completeness we note that other single-field regimes (for example ultra-slow-roll or constant-roll) alter both background and perturbation dynamics in different ways; representative studies include [101–104]. A full treatment of these alternative regimes is beyond the present paper but would be interesting for future work.

B. Implementation of higher-order slow-roll approximations

In the previous section, we estimated the reheating parameters and e-folding number using the numerical background solution with the leading-order inflationary observables, i.e., Eqs. (16). However, as mentioned earlier, these expressions are obtained using leading-order slow-roll, and the full solutions of the amplitude of scalar power spectrum, scalar spectral index as well as the tensor-to-scalar ratio in terms of the slow-roll parameter are given as [25, 76]:

$$A_s = 1 - 2(C+1)\epsilon_1 - C\epsilon_2 + \left(2C^2 + 2C + \frac{\pi^2}{2} - f\right)\epsilon_1^2 + \left(C^2 - C + \frac{7\pi^2}{12} - g\right)\epsilon_1\epsilon_2 + \left(\frac{1}{2}C^2 + \frac{\pi^2}{8} - 1\right)\epsilon_2^2 + \left(-\frac{1}{2}C^2 + \frac{\pi^2}{24}\right)\epsilon_2\epsilon_3, \quad (38)$$

$$n_s = 1 - 2\epsilon_1 - \epsilon_2 - 2\epsilon_1^2 - (3 + 2C)\epsilon_1\epsilon_2 - C\epsilon_2\epsilon_3, \quad (39)$$

$$r = 16\epsilon_1\left(1 + 2C\frac{\epsilon_2}{2}\right), \quad (40)$$

	Analytical approximations	Numerical solution
$w_{\text{re}} < 1/3$	$52 \leq N_k \leq 56,$ $0.9613 \leq n_s \leq 0.9641$ $N_{\text{re}} \leq 16 (w_{\text{re}} = 0),$ $T_{\text{re}} \geq 10^{10} \text{ GeV} (w_{\text{re}} = 0)$	$50 \leq N_k \leq 56,$ $0.9613 \leq n_s \leq 0.9649,$ $N_{\text{re}} \leq 21 (w_{\text{re}} = 0),$ $T_{\text{re}} \geq 10^8 \text{ GeV} (w_{\text{re}} = 0)$
$w_{\text{re}} > 1/3$	$56 \leq N_k \leq 74,$ $0.9641 \leq n_s \leq 0.9731,$ $N_{\text{re}} \leq 37 (w_{\text{re}} = 1),$ $T_{\text{re}} \geq 10^{-9} \text{ GeV} (w_{\text{re}} = 1)$	$56 \leq N_k \leq 73,$ $0.9649 \leq n_s \leq 0.9731,$ $N_{\text{re}} \leq 34 (w_{\text{re}} = 1),$ $T_{\text{re}} \geq 10^{-8} \text{ GeV} (w_{\text{re}} = 1)$
future observations ($w_{\text{re}} > 1/3$: allowed) ($w_{\text{re}} < 1/3$: not allowed)	$59 \leq N_k \leq 63,$ $0.9662 \leq n_s \leq 0.9682,$ $7 \leq N_{\text{re}} \leq 14 (w_{\text{re}} = 1),$ $10^9 \text{ GeV} \geq T_{\text{re}} \geq 10^6 \text{ GeV} (w_{\text{re}} = 1)$	$58 \leq N_k \leq 62,$ $0.9662 \leq n_s \leq 0.9682,$ $4 \leq N_{\text{re}} \leq 12 (w_{\text{re}} = 1),$ $10^{12} \text{ GeV} \geq T_{\text{re}} \geq 10^7 \text{ GeV} (w_{\text{re}} = 1)$

TABLE I. Starobinsky Inflation: The bounds on variables N_k , n_s , N_{re} , and T_{re} for different values of w_{re} corresponding to analytically (slow-roll) approximated and the numerical solutions are shown.

where $C = -2 + \ln 2 + \gamma$, and γ is the Euler constant, $f = 5$ and $g = 7$. Here, all slow-roll parameters are evaluated using the full numerical background solution. In this section, instead of using Eqs. (16), along with the numerical solution, we consider the above expressions for the observable, repeat the reheating analysis, and compare our results with the numerical results obtained in the previous section, which has been illustrated in Figs. 6 and 7 as well as in Table II.

As can be seen again in Fig. 6, there is a further shift in reheating parameters, N_{re} and T_{re} compared to the improvements mentioned in the previous section. We obtain an additional improvement of $\Delta n_s \sim 4 \times 10^{-4}$, resulting in a new bound on n_s , namely $n_s \leq 0.9653$ for $w_{\text{re}} < 1/3$. Thus, considering higher-order slow-roll approximations instead of the leading-order leads to an additional correction of order 4×10^{-4} , further refining the theoretical predictions. The detailed bounds on parameters are shown in the Table II.

To understand this physically, recall that the scalar spectral index is evaluated at the moment the pivot scale $k_* = 0.05 \text{ Mpc}^{-1}$ crosses the Hubble horizon during inflation, i.e. at $k_* = a_* H_*$. At this moment, the slow-roll parameters ϵ_1 and ϵ_2 are already non-zero — for the Starobinsky

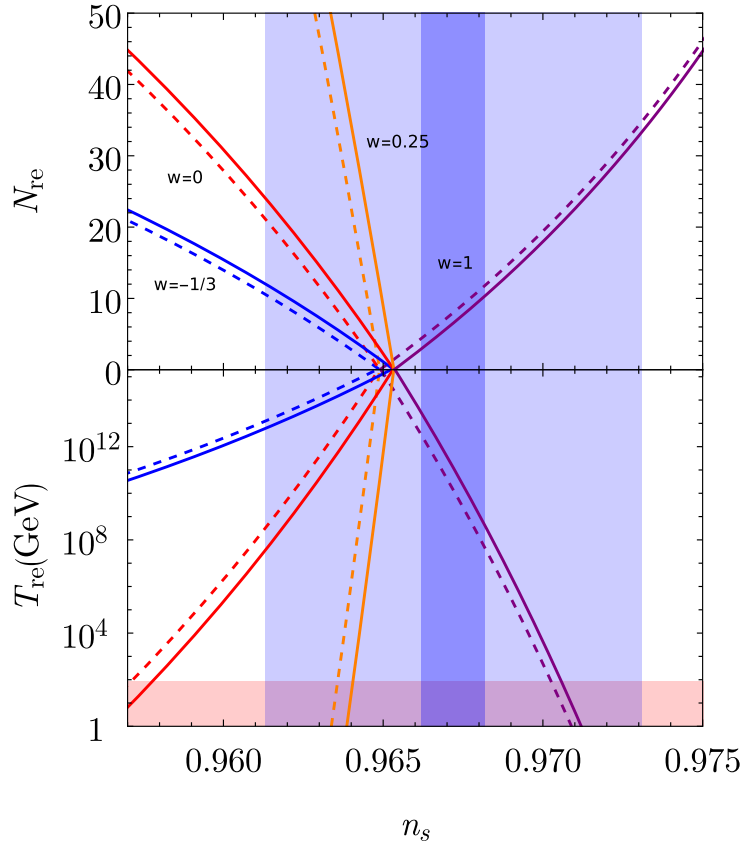


FIG. 6. We plot the duration of reheating N_{re} and reheating temperature T_{re} given by Eqs. (24) and (25) as functions of the scalar spectral index n_s parametrically comparing numerical solution with leading-order approximations and numerical solution with higher-order approximations given by Eq. (16), (39) respectively. The solid lines are for the higher-order approximations and the dashed lines are for the leading-order approximations. Please note that different colors represent dynamics corresponding to different effective equations of state parameter w_{re} as indicated in the figure. The blue-shaded region represents the 1σ constraint on the value of n_s using ongoing observations [32–35] with $n_s = 0.9672 \pm 0.0059$. The dark blue region shows the future projected bound on n_s with a sensitivity of 10^{-3} , assuming its central value remains unchanged. The temperature below the lighter red region is excluded due to the constraint from the electroweak scale, which is taken to be 100 GeV.

model with $N_k \sim 55$, one finds $\epsilon_1 \sim 10^{-3}$ and $\epsilon_2 \sim 2/N_k \sim 0.036$. Truncating the perturbation spectrum at leading-order ($n_s \simeq 1 - 2\epsilon_1 - \epsilon_2$) therefore neglects contributions of order ϵ_1^2 , $\epsilon_1\epsilon_2$, ϵ_2^2 , and ϵ_3 , which are not identically zero at horizon crossing. The higher-order corrections [105] systematically account for these terms, tightening the prediction for n_s . The resulting shift of $\sim 4 \times 10^{-4}$ is subdominant compared to the numerical background correction ($\sim 10^{-3}$) but is nonetheless at the threshold of detectability for next-generation CMB experiments.

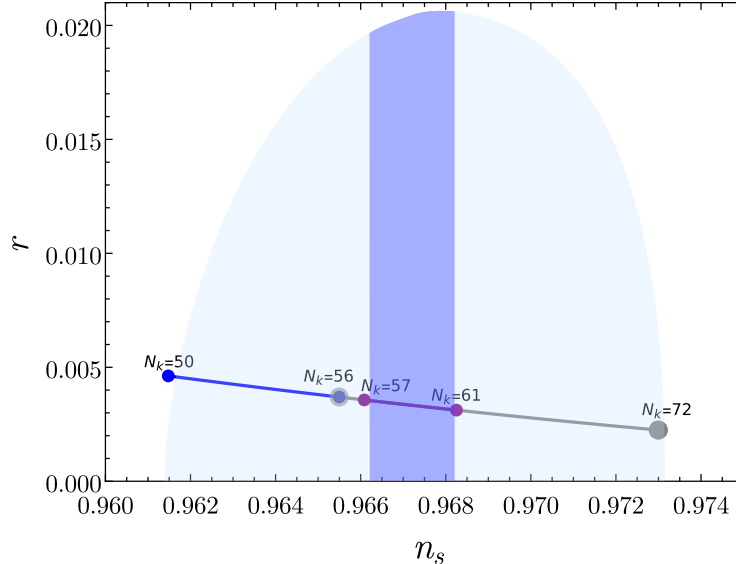


FIG. 7. We plot the inflationary observables, tensor-to-scalar ratio (r) as a function of scalar spectral index (n_s) for the Starobinsky model using higher-order approximations given by Eq. (39) and (40). This evolution is presented considering the bound on duration N_k using the reheating regime. We consider different EoS parameters during reheating w_{re} and observe the constraint on the duration N_k . Correspondingly, in the figure, blue line corresponds to the bound for $w_{\text{re}} < 1/3$, the gray line for $w_{\text{re}} > 1/3$ and the purple line for the future observational bound of n_s . The blue-shaded region represents the 1σ constraint on the value of n_s using ongoing observations [32–35] with $n_s = 0.9672 \pm 0.0059$. The dark blue region shows the future projected bound on n_s with a sensitivity of 10^{-3} , assuming its central value remains unchanged.

C. Implementation of the onset of reheating as the bottom of the potential

Thus far, we were estimating N_{re} and T_{re} , considering the onset of the reheating era after the end of inflation. However, in Ref. [63], it has been shown that, instead of considering minimal gravity theory, if one considers modified gravity theories, the onset of reheating as the end of inflation can make a significant change in the analysis. This is because, ϵ_1 is not an invariant under conformal transformation. Therefore, in a meaningful manner, one can choose the onset of reheating as the bottom of the potential, as this point is conformally invariant, and can be used even for general modified gravity theories. Therefore, in this section, we introduce corrections to the reheating analysis, and thus the observables, by considering that the reheating era commences after the epoch at which the potential touches its minima (bottom of the potential). In that case,

	Numerical solution with leading-order n_s, r expressions	Numerical solution with higher-order n_s, r expressions
$w_{\text{re}} < 1/3$	$50 \leq N_k \leq 56,$ $0.9613 \leq n_s \leq 0.9649$ $N_{\text{re}} \leq 21 (w_{\text{re}} = 0),$ $T_{\text{re}} \geq 10^8 \text{ GeV} (w_{\text{re}} = 0)$	$50 \leq N_k \leq 56,$ $0.9613 \leq n_s \leq 0.9653,$ $N_{\text{re}} \leq 24 (w_{\text{re}} = 0),$ $T_{\text{re}} \geq 10^7 \text{ GeV} (w_{\text{re}} = 0)$
$w_{\text{re}} > 1/3$	$56 \leq N_k \leq 73,$ $0.9649 \leq n_s \leq 0.9731,$ $N_{\text{re}} \leq 34 (w_{\text{re}} = 1),$ $T_{\text{re}} \geq 10^{-8} \text{ GeV} (w_{\text{re}} = 1)$	$56 \leq N_k \leq 72,$ $0.9653 \leq n_s \leq 0.9731,$ $N_{\text{re}} \leq 33 (w_{\text{re}} = 1),$ $T_{\text{re}} \geq 10^{-7} \text{ GeV} (w_{\text{re}} = 1)$
future observations ($w_{\text{re}} > 1/3$: allowed) ($w_{\text{re}} < 1/3$: not allowed)	$58 \leq N_k \leq 62,$ $0.9662 \leq n_s \leq 0.9682,$ $4 \leq N_{\text{re}} \leq 12 (w_{\text{re}} = 1),$ $10^{12} \text{ GeV} \geq T_{\text{re}} \geq 10^7 \text{ GeV} (w_{\text{re}} = 1)$	$57 \leq N_k \leq 61,$ $0.9662 \leq n_s \leq 0.9682,$ $3 \leq N_{\text{re}} \leq 10 (w_{\text{re}} = 1),$ $10^{13} \text{ GeV} \geq T_{\text{re}} \geq 10^8 \text{ GeV} (w_{\text{re}} = 1)$

TABLE II. Starobinsky Inflation: The bounds on variables N_k , n_s , N_{re} , and T_{re} for different values of w_{re} corresponding to leading-order approximations and the higher-order approximations are shown. Note that, in both cases, the background solutions are numerically obtained.

Eq. (24) can be re-written as

$$N_{\text{re}} = \frac{4}{1-3w_{\text{re}}} \left[-N_k - N_{\text{eb}} - \frac{1}{4} \ln \left(\frac{30}{\pi^2 g_{\text{reh}}} \right) - \frac{1}{3} \ln \left(\frac{11g_{\text{s,re}}}{43} \right) - \ln \left(\frac{k}{a_0 T_0} \right) - \frac{1}{4} \ln \left(\frac{\rho_{\text{b}}}{H_k^4} \right) \right], \quad (41)$$

and the reheating temperature, i.e., Eq. (25) can also be evaluated as:

$$T_{\text{re}} = \frac{a_0 T_0}{k} \left(\frac{43}{11g_{\text{s,re}}} \right) e^{-N_k - N_{\text{eb}} - N_{\text{re}}}. \quad (42)$$

Here, $N_{\text{eb}} \equiv \ln(a_{\text{b}}/a_{\text{end}})$ and $\rho_{\text{b}} \equiv 3H_{\text{b}}^2$, where (b) denotes the bottom of the potential. Again, we perform our analysis considering the numerically obtained solution with higher-order slow-roll corrections and the onset of reheating as the bottom of the potential. However, to our surprise, we find that this implementation does not improve the accuracy to a significant amount, as $\Delta n_s \sim$

10^{-5} . This small correction reflects the fact that, in minimally coupled models, the difference between the end of inflation and the minimum of the potential is dynamically short.

This small contribution can be understood as follows. The reheating onset determines the initial value of $\rho_{\text{re},i}$ used in the computation of N_{re} via Eq. (24). When the onset is shifted from ϕ_{end} (where $\epsilon_1 = 1$) to ϕ_b (where $V'(\phi_b) = 0$, the potential minimum), the inflaton has already transferred a fraction of its energy to oscillations. However, for the Starobinsky potential, the ratio $\rho_{\text{end}}/\rho_b \simeq 1 + \mathcal{O}(\epsilon_1^2)$ at the transition point, meaning the energy difference between these two definitions is at most second order in slow-roll. Since $N_{\text{re}} \propto \ln(\rho_{\text{re},i}/\rho_{\text{re},f})$, the logarithmic sensitivity of N_{re} to the initial condition suppresses the shift further, resulting in a negligible $\Delta n_s \sim 10^{-5}$. This confirms that while careful treatment of the reheating *onset* is conceptually important, the dominant source of theoretical uncertainty lies in the accurate determination of ρ_{end} through the full numerical background evolution.

To summarize our cumulative result, in Fig. 8, we plot the results obtained through the analytical approximations mentioned in the first section and the improvement obtained through the implementation of three corrections to the dynamics, and Table III summarizes the cumulative effect of all corrections relative to the purely analytical treatment. Compared to the purely analytical slow-roll treatment presented in Sec. III, the cumulative implementation of these corrections results in a maximum shift of $\Delta n_s \sim 1.2 \times 10^{-3}$ within the allowed reheating range. This shift is evaluated relative to the leading-order slow-roll prediction at fixed reheating assumptions. Note that, if the central value of n_s is assumed to be ~ 0.9672 even in this case, then even with the improvements, the Starobinsky model would be disfavored at the 1σ level from the expected future observation. Although illustrated using the Starobinsky model, similar end-of-inflation corrections are expected in any inflationary model where slow-roll breaks down near the end of inflation.

It is instructive to compare the present results quantitatively with prior treatments of the Starobinsky model in the literature. Within the standard analytical slow-roll approximation $n_s \simeq 1 - 2/N_k$, the leading-order treatments of Cook et al. [50] and Martin & Ringeval [44] yield $n_s \leq 0.9641$ for $w_{\text{re}} < 1/3$, corresponding to $N_k \leq 56$, and $N_{\text{re}} \leq 16$, $T_{\text{re}} \geq 10^{10}$ GeV for $w_{\text{re}} = 0$, as reproduced in our Table III (left column). Our improved framework — incorporating full numerical background evolution, higher-order slow-roll corrections, and a revised onset of reheating at the potential minimum — shifts this upper bound to $n_s \leq 0.9653$, corresponding to $N_{\text{re}} \leq 24$ and $T_{\text{re}} \geq 10^7$ GeV for $w_{\text{re}} = 0$ (Table III, right column), a cumulative upward shift of $\Delta n_s \sim 1.2 \times 10^{-3}$. A related refinement in the same direction was recently reported by Drees & Xu [106], who derive

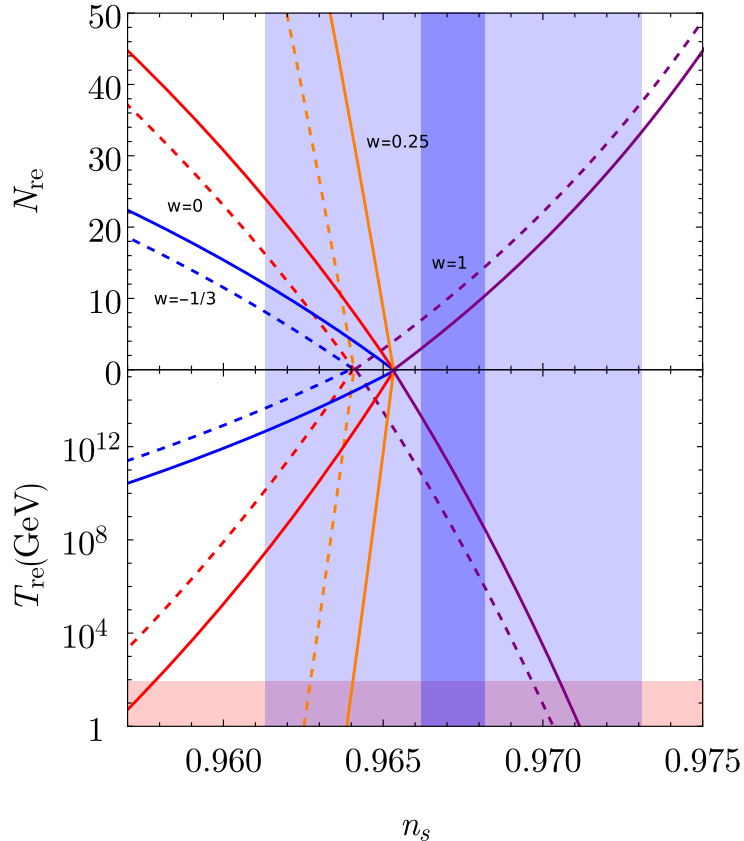


FIG. 8. We plot the duration of reheating N_{re} and reheating temperature T_{re} given by Eqs. (24) and (25) as functions of the scalar spectral index n_s parametrically comparing analytically approximated solution and numerical background solution with higher-order slow-roll corrections, given by Eqs. (31), (39) respectively. The solid lines are for the onset of reheating as the bottom of the potential and the dashed lines are for the analytically approximated solution. Please note that different colors represent dynamics corresponding to different effective equations of state parameter w_{re} as indicated in the figure. The blue-shaded region represents the 1σ constraint on the value of n_s using ongoing observations [32–35] with $n_s = 0.9672 \pm 0.0059$. The dark blue region shows the future projected bound on n_s with a sensitivity of 10^{-3} , assuming its central value remains unchanged. The temperature below the lighter red region is excluded due to the constraint from the electroweak scale, which is taken to be 100 GeV.

an improved analytical approximation

$$n_s \simeq 1 - \frac{2}{N_\star - \frac{3}{4} \ln\left(\frac{2}{N_\star}\right)}, \quad (43)$$

and demonstrate that the standard expression $n_s \simeq 1 - 2/N_k$ systematically underestimates n_s for the Starobinsky model, consistent with the direction of our corrections. However, unlike that work, the present analysis employs a full numerical integration of the background equations (Eqs. (9) and

(10)) and additionally decomposes each correction individually: the numerical background treatment alone contributes $\Delta n_s \sim 10^{-3}$, higher-order slow-roll corrections add a further $\sim 4 \times 10^{-4}$, and the revised onset of reheating contributes negligibly at $\sim 10^{-5}$. For $w_{re} > 1/3$, the upper bound on N_k shifts from $N_k \leq 74$ (analytical) to $N_k \leq 72$ (corrected), while the corresponding lower bound on n_s shifts from 0.9641 to 0.9653. The correction $\Delta n_s \sim 10^{-3}$ is comparable in magnitude to the projected sensitivity of forthcoming experiments such as PRISM [65], EUCLID [66], CORE [68], and cosmic 21-cm surveys [67], underscoring that theoretical precision at this level is indispensable for unambiguous model discrimination in the next generation of CMB observations. To our knowledge, a systematic decomposition of end-of-inflation corrections and their explicit propagation into n_s has not been reported in prior reheating analyses of the Starobinsky model. These are the main results of this work.

This demonstrates that theoretical control at the $\mathcal{O}(10^{-3})$ level is necessary for robust model discrimination: models marginally accepted or excluded under leading-order slow-roll predictions may move across acceptance boundaries once end-of-inflation corrections are included. A dedicated forecast that folds our Δn_s corrections into Fisher- or MCMC-based model-selection would be a valuable follow-up study.

V. SUMMARY AND CONCLUSIONS

In this article, we consider a single canonical scalar field model minimally coupled to the gravity with a potential $V(\phi)$ that drives the evolution of the early universe, including both slow-roll inflation and oscillatory solution around the minimum of the potential, also known as the reheating epoch. In obtaining the solution, we often use different sets of approximations in both regimes. In the slow-roll inflationary regime, where $\epsilon_1, \epsilon_2 \ll 1$, we rely upon the slow-roll approximations. In contrast, the reheating epoch is, for simplicity, quantitatively characterized by the effective EoS parameter w_{re} and the duration of this epoch N_{re} (or the reheating temperature T_{re}). However, these approximations may lead to a significant discrepancy in the theoretical estimation of the observables (n_s and r). While accurately defining the reheating epoch (*viz.* the qualitative analysis) is challenging, this work focuses on examining the impact of a more accurate dynamics, rather than the slow-roll approximations, on the perturbed observables.

In order to do this, we specifically considered the following improvements in the dynamics:

	Analytical approximations	Higher-order approximations
$w_{\text{re}} < 1/3$	$52 \leq N_k \leq 56,$ $0.9613 \leq n_s \leq 0.9641,$ $N_{\text{re}} \leq 16 (w_{\text{re}} = 0),$ $T_{\text{re}} \geq 10^{10} \text{ GeV} (w_{\text{re}} = 0)$	$50 \leq N_k \leq 56,$ $0.9613 \leq n_s \leq 0.9653,$ $N_{\text{re}} \leq 24 (w_{\text{re}} = 0),$ $T_{\text{re}} \geq 10^7 \text{ GeV} (w_{\text{re}} = 0)$
$w_{\text{re}} > 1/3$	$56 \leq N_k \leq 74,$ $0.9641 \leq n_s \leq 0.9731,$ $N_{\text{re}} \leq 37 (w_{\text{re}} = 1),$ $T_{\text{re}} \geq 10^{-9} \text{ GeV} (w_{\text{re}} = 1)$	$56 \leq N_k \leq 72,$ $0.9653 \leq n_s \leq 0.9731,$ $N_{\text{re}} \leq 33 (w_{\text{re}} = 1),$ $T_{\text{re}} \geq 10^{-7} \text{ GeV} (w_{\text{re}} = 1)$
future observations ($w_{\text{re}} > 1/3$: allowed) ($w_{\text{re}} < 1/3$: not allowed)	$59 \leq N_k \leq 63,$ $0.9662 \leq n_s \leq 0.9682,$ $7 \leq N_{\text{re}} \leq 14 (w_{\text{re}} = 1),$ $10^9 \text{ GeV} \geq T_{\text{re}} \geq 10^6 \text{ GeV} (w_{\text{re}} = 1)$	$57 \leq N_k \leq 61,$ $0.9662 \leq n_s \leq 0.9682,$ $3 \leq N_{\text{re}} \leq 10 (w_{\text{re}} = 1),$ $10^{13} \text{ GeV} \geq T_{\text{re}} \geq 10^8 \text{ GeV} (w_{\text{re}} = 1)$

TABLE III. Starobinsky Inflation: The bounds on variables, N_k , n_s , N_{re} , and T_{re} for different values of w_{re} corresponding to analytical approximated parameters, and numerical solution with higher-order approximations are shown.

1. Numerical Solution: In this method, we solve the complete background Eq. (10) using the numerical method, which provides us with an accurate solution for the dynamics of the universe in its early phase. Using this solution, we estimate the observables and compare the results with the solutions obtained using slow-roll approximation.
2. Higher-order approximations: This method includes higher-order slow-roll corrections to the inflationary observables, Eqs. (38), (39) and (40), rather than Eqs. (16). Here also, we used complete numerical solution and estimated the observables using higher-order slow-roll corrections and estimated the discrepancy in the observables with respect to the analytical solution obtained using slow-roll approximation.
3. Onset of the reheating as the bottom of the potential: Typically, the end of inflation is considered the onset of the reheating epoch. However, in this method, we show that if reheating begins at the bottom of the potential, the reheating parameters are modified, as

given by Eq. (41) and Eq. (42). This modification can provide a new bound on the duration N_k , leading to a discrepancy in the scalar spectral index.

After implementing these changes, we found an improvement in the theoretical bounds on the observables. As seen in Fig. 8, there is an improvement of $\Delta n_s \sim 1.2 \times 10^{-3}$. These numerical predictions indicate that for $w_{\text{re}} < 1/3$, the Starobinsky model has an upper bound as $n_s \leq 0.9653$. This can be disfavored from the future observational constraint if the central value is $n_s \simeq 0.9672$ [35]. However, for $w_{\text{re}} > 1/3$, the reheating parameters fall within the future observational bounds, though, at the cost of sufficient reheating e-folding number ($\sim \mathcal{O}(1 - 2)$). This scenario would be strongly constrained if future observations favor instantaneous reheating [99, 100].

Physically, these corrections share a common origin: the standard slow-roll approximation is inherently perturbative and assumes that $\epsilon_i \ll 1$ throughout inflation. However, all three corrections become relevant precisely in the regime where this assumption weakens — near the end of inflation where $\epsilon_1 \rightarrow 1$ (numerical correction), at horizon crossing where $\epsilon_2 \not\ll 1$ (higher-order correction), and at the transition to the oscillatory phase (onset correction). The Starobinsky model, with its characteristic plateau potential, is particularly sensitive to these effects because the slow-roll parameters evolve rapidly in the final $\mathcal{O}(1)$ e-fold before inflation ends. Models with similarly steep exit from the inflationary plateau — such as α -attractors and Higgs inflation — are expected to exhibit corrections of comparable magnitude, making the present analysis broadly relevant beyond the specific case studied here. By contrast, models whose exit dynamics are much smoother or whose reheating is driven by qualitatively different microphysics (small-field models with very flat exits, or scenarios with early preheating) may show smaller or model-dependent shifts. A practical conclusion is that the numerical re-evaluation we propose is straightforward to apply model-by-model, and should be performed when aiming for theoretical predictions at $\mathcal{O}(10^{-3})$ precision.

These results demonstrate that an accurate theoretical treatment of end-of-inflation dynamics is as essential as higher-order perturbative corrections in precision-era inflationary analyses. Even corrections that are often regarded as subleading can induce observable shifts in perturbed quantities, and therefore must be systematically incorporated when deriving constraints on inflationary models. While the present work focuses on slow-roll dynamics within a minimal framework, further refinements — including a more detailed reheating treatment, higher-order correlations such as non-Gaussianity [107–109], the role of primordial black holes and gravitational waves, extensions to non-minimal gravity [110], and alternative early-universe scenarios such as viable classical

bounces [111–116] — may further sharpen theoretical predictions. It would also be valuable to extend our numerical framework to warm inflation (introducing a dissipation term $\Gamma(\phi, T)$ and a coupled radiation component) and quantify whether dissipative dynamics amplify or suppress the $\Delta n_s \sim 10^{-3}$ correction found here for cold inflation. Such a direct warm-cold comparison will show whether both paradigms produce comparable-order shifts in observables or whether dissipation qualitatively changes the sensitivity to end-of-inflation modelling. A careful and consistent implementation of such effects remains an important direction for future investigations.

ACKNOWLEDGEMENTS

DN is supported by the DST, Government of India through the DST-INSPIRE Faculty fellowship (04/2020/002142). MK is supported by a DST-INSPIRE Fellowship under the reference number: IF170808, DST, Government of India. D.N. is grateful to the Department of Physics, School of Advanced Sciences, Vellore Institute of Technology (VIT) Chennai, for institutional support and academic encouragement. DN, SY and MK are also very thankful to the Department of Physics and Astrophysics, University of Delhi. MK, SY and DN also acknowledge facilities provided by the IUCAA Centre for Astronomy Research and Development (ICARD), University of Delhi.

-
- [1] A. A. Starobinsky, *JETP Lett.* **30**, 682 (1979).
 - [2] A. A. Starobinsky, *Phys. Lett. B* **91**, 99 (1980).
 - [3] A. H. Guth, *Phys. Rev. D* **23**, 347 (1981).
 - [4] K. Sato, *Monthly Notices of the Royal Astronomical Society* **195**, 467 (1981), <http://oup.prod.sis.lan/mnras/article-pdf/195/3/467/4065201/mnras195-0467.pdf>.
 - [5] V. F. Mukhanov and G. V. Chibisov, *JETP Lett.* **33**, 532 (1981), [*Pisma Zh. Eksp. Teor. Fiz.*33,549(1981)].
 - [6] A. Linde, *Physics Letters B* **108**, 389 (1982).
 - [7] S. Hawking, *Physics Letters B* **115**, 295 (1982).
 - [8] A. A. Starobinsky, *Phys. Lett. B* **117**, 175 (1982).
 - [9] A. H. Guth and S.-Y. Pi, *Phys. Rev. Lett.* **49**, 1110 (1982).
 - [10] M. Sasaki, *Progress of Theoretical Physics* **76**, 1036 (1986).
 - [11] A. Albrecht and P. J. Steinhardt, *Phys. Rev. Lett.* **48**, 1220 (1982).
 - [12] A. D. Linde, *Phys. Lett.* **129B**, 177 (1983).
 - [13] A. Vilenkin, *Nuclear Physics B* **226**, 527 (1983).

- [14] J. M. Bardeen, P. J. Steinhardt, and M. S. Turner, *Phys. Rev. D* **28**, 679 (1983).
- [15] E. W. Kolb and M. Turner, *The early universe* (Reading, Mass. : Addison-Wesley, 1990).
- [16] V. F. Mukhanov, H. A. Feldman, and R. H. Brandenberger, *Phys. Rept.* **215**, 203 (1992).
- [17] A. R. Liddle, P. Parsons, and J. D. Barrow, *Phys. Rev. D* **50**, 7222 (1994), arXiv:astro-ph/9408015.
- [18] J. E. Lidsey, A. R. Liddle, E. W. Kolb, E. J. Copeland, T. Barreiro, *et al.*, *Rev.Mod.Phys.* **69**, 373 (1997), arXiv:astro-ph/9508078 [astro-ph].
- [19] E. J. Copeland, A. R. Liddle, and D. Wands, *Phys. Rev. D* **57**, 4686 (1998), arXiv:gr-qc/9711068.
- [20] J. Martin and R. H. Brandenberger, *Phys. Rev. D* **63**, 123501 (2001), arXiv:hep-th/0005209.
- [21] A. Linde, arXiv e-prints , hep-th/0503203 (2005), arXiv:hep-th/0503203 [astro-ph].
- [22] D. H. Lyth, *22nd IAP Colloquium on Inflation + 25: The First 25 Years of Inflationary Cosmology Paris, France, June 26-30, 2006*, *Lect. Notes Phys.* **738**, 81 (2008), arXiv:hep-th/0702128 [hep-th].
- [23] L. Sriramkumar, (2009), arXiv:0904.4584 [astro-ph.CO].
- [24] D. Baumann, in *Physics of the large and the small, TASI 09, proceedings of the Theoretical Advanced Study Institute in Elementary Particle Physics, Boulder, Colorado, USA, 1-26 June 2009* (2011) pp. 523–686, arXiv:0907.5424 [hep-th].
- [25] J. Martin, C. Ringeval, and V. Vennin, *Phys. Dark Univ.* **5-6**, 75 (2014), arXiv:1303.3787 [astro-ph.CO].
- [26] A. Linde, in *Proceedings, 100th Les Houches Summer School: Post-Planck Cosmology: Les Houches, France, July 8 - August 2, 2013* (2015) pp. 231–316, arXiv:1402.0526 [hep-th].
- [27] J. Martin, *Astrophys. Space Sci. Proc.* **45**, 41 (2016), arXiv:1502.05733 [astro-ph.CO].
- [28] P. Ade *et al.* (Planck), *Astron. Astrophys.* **594**, A20 (2016), arXiv:1502.02114 [astro-ph.CO].
- [29] P. Ade *et al.* (Planck), *Astron. Astrophys.* **594**, A17 (2016), arXiv:1502.01592 [astro-ph.CO].
- [30] S. Clesse, in *10th Modave Summer School in Mathematical Physics* (2015) arXiv:1501.00460 [astro-ph.CO].
- [31] S. D. Odintsov, V. K. Oikonomou, I. Giannakoudi, F. P. Fronimos, and E. C. Lympieriadou, *Symmetry* **15**, 1701 (2023), arXiv:2307.16308 [gr-qc].
- [32] Y. Akrami *et al.* (Planck), *Astron. Astrophys.* **641**, A10 (2020), arXiv:1807.06211 [astro-ph.CO].
- [33] N. Aghanim *et al.* (Planck), *Astron. Astrophys.* **641**, A6 (2020), [Erratum: *Astron.Astrophys.* 652, C4 (2021)], arXiv:1807.06209 [astro-ph.CO].
- [34] P. A. R. Ade *et al.* (BICEP, Keck), *Phys. Rev. Lett.* **127**, 151301 (2021), arXiv:2110.00483 [astro-ph.CO].
- [35] G. Galloni, N. Bartolo, S. Matarrese, M. Migliaccio, A. Ricciardone, and N. Vittorio, *JCAP* **04**, 062, arXiv:2208.00188 [astro-ph.CO].
- [36] A. Albrecht, P. J. Steinhardt, M. S. Turner, and F. Wilczek, *Phys. Rev. Lett.* **48**, 1437 (1982).
- [37] L. F. Abbott, E. Farhi, and M. B. Wise, *Phys. Lett.* **117B**, 29 (1982).
- [38] J. H. Traschen and R. H. Brandenberger, *Phys. Rev. D* **42**, 2491 (1990).

- [39] L. Kofman, A. D. Linde, and A. A. Starobinsky, *Phys. Rev. Lett.* **73**, 3195 (1994), arXiv:hep-th/9405187 [hep-th].
- [40] Y. Shtanov, J. H. Traschen, and R. H. Brandenberger, *Phys. Rev. D* **51**, 5438 (1995), arXiv:hep-ph/9407247.
- [41] L. Kofman, A. D. Linde, and A. A. Starobinsky, *Phys. Rev.* **D56**, 3258 (1997), arXiv:hep-ph/9704452 [hep-ph].
- [42] B. A. Bassett, S. Tsujikawa, and D. Wands, *Rev. Mod. Phys.* **78**, 537 (2006), arXiv:astro-ph/0507632 [astro-ph].
- [43] R. Allahverdi, R. Brandenberger, F.-Y. Cyr-Racine, and A. Mazumdar, *Ann. Rev. Nucl. Part. Sci.* **60**, 27 (2010), arXiv:1001.2600 [hep-th].
- [44] J. Martin and C. Ringeval, *Phys. Rev.* **D82**, 023511 (2010), arXiv:1004.5525 [astro-ph.CO].
- [45] J. Mielczarek, *Phys. Rev. D* **83**, 023502 (2011), arXiv:1009.2359 [astro-ph.CO].
- [46] M. A. Amin, M. P. Hertzberg, D. I. Kaiser, and J. Karouby, *Int. J. Mod. Phys.* **D24**, 1530003 (2014), arXiv:1410.3808 [hep-ph].
- [47] L. Dai, M. Kamionkowski, and J. Wang, *Phys. Rev. Lett.* **113**, 041302 (2014), arXiv:1404.6704 [astro-ph.CO].
- [48] J. Martin, C. Ringeval, and V. Vennin, *Phys. Rev. Lett.* **114**, 081303 (2015), arXiv:1410.7958 [astro-ph.CO].
- [49] V. Domcke and J. Heisig, *Phys. Rev. D* **92**, 103515 (2015), arXiv:1504.00345 [astro-ph.CO].
- [50] J. L. Cook, E. Dimastrogiovanni, D. A. Easson, and L. M. Krauss, *JCAP* **1504**, 047, arXiv:1502.04673 [astro-ph.CO].
- [51] D. Maity and P. Saha, (2016), arXiv:1610.00173 [astro-ph.CO].
- [52] K. D. Lozanov and M. A. Amin, *Phys. Rev. Lett.* **119**, 061301 (2017), arXiv:1608.01213 [astro-ph.CO].
- [53] R. Kabir, A. Mukherjee, and D. Lohiya, *Mod. Phys. Lett. A* **34**, 1950114 (2019), arXiv:1609.09243 [gr-qc].
- [54] D. Maity and P. Saha, (2018), arXiv:1811.11173 [astro-ph.CO].
- [55] D. Maity and P. Saha, *Class. Quant. Grav.* **36**, 045010 (2019), arXiv:1902.01895 [gr-qc].
- [56] K. El Bourakadi, (2021), arXiv:2104.10552 [gr-qc].
- [57] S. D. Odintsov and T. Paul, *Phys. Dark Univ.* **42**, 101263 (2023), arXiv:2305.19110 [gr-qc].
- [58] G. German, J. C. Hidalgo, and L. E. Padilla, *Eur. Phys. J. Plus* **139**, 302 (2024), arXiv:2310.05221 [astro-ph.CO].
- [59] J. B. Munoz and M. Kamionkowski, *Phys. Rev. D* **91**, 043521 (2015), arXiv:1412.0656 [astro-ph.CO].
- [60] J. Martin and C. Ringeval, *JCAP* **0608**, 009, arXiv:astro-ph/0605367 [astro-ph].
- [61] P. Adshead, R. Easther, J. Pritchard, and A. Loeb, *JCAP* **02**, 021, arXiv:1007.3748 [astro-ph.CO].
- [62] J.-O. Gong, S. Pi, and G. Leung, *JCAP* **1505** (05), 027, arXiv:1501.03604 [hep-ph].
- [63] D. Nandi and P. Saha, (2019), arXiv:1907.10295 [gr-qc].
- [64] A. R. Liddle and S. M. Leach, *Phys. Rev.* **D68**, 103503 (2003), arXiv:astro-ph/0305263 [astro-ph].

- [65] P. Andre *et al.* (PRISM), (2013), [arXiv:1306.2259 \[astro-ph.CO\]](#).
- [66] L. Amendola *et al.* (Euclid Theory Working Group), *Living Rev. Rel.* **16**, 6 (2013), [arXiv:1206.1225 \[astro-ph.CO\]](#).
- [67] Y. Mao, M. Tegmark, M. McQuinn, M. Zaldarriaga, and O. Zahn, *Phys. Rev.* **D78**, 023529 (2008), [arXiv:0802.1710 \[astro-ph\]](#).
- [68] F. Finelli *et al.* (CORE), *JCAP* **1804**, 016, [arXiv:1612.08270 \[astro-ph.CO\]](#).
- [69] A. Jawad, N. Azhar, S. Sadiq, and S. Rani, *Chin. Phys. C* **48**, 095107 (2024).
- [70] S. Maqsood, A. Jawad, and N. Videla, *Phys. Dark Univ.* **33**, 100865 (2021).
- [71] S. Rani, F. Rasool, A. Jawad, and A. M. Sultan, *Chin. J. Phys.* **90**, 788 (2024).
- [72] A. D. Alruwaili, A. Jawad, and S. Sadiq, *Phys. Dark Univ.* **51**, 102188 (2026).
- [73] S. Qummer, A. Jawad, and M. Younas, *Astropart. Phys.* **133**, 102626 (2021).
- [74] M. Kaur, D. Nandi, and S. R. B, *JCAP* **05**, 045, [arXiv:2309.10570 \[astro-ph.CO\]](#).
- [75] P. Auclair, B. Blachier, and C. Ringeval, (2024), [arXiv:2406.14152 \[astro-ph.CO\]](#).
- [76] Q.-G. Huang, *Phys. Rev. D* **76**, 043505 (2007), [arXiv:astro-ph/0610924](#).
- [77] C. Caprini, S. H. Hansen, and M. Kunz, *Mon. Not. Roy. Astron. Soc.* **339**, 212 (2003), [arXiv:hep-ph/0210095](#).
- [78] J. M. Cline and L. Hoi, *JCAP* **06**, 007, [arXiv:astro-ph/0603403](#).
- [79] Q.-G. Huang and M. Li, *Nucl. Phys. B* **755**, 286 (2006), [arXiv:astro-ph/0603782](#).
- [80] Q.-G. Huang, *JCAP* **11**, 004, [arXiv:astro-ph/0610389](#).
- [81] H. Peiris and R. Easther, *JCAP* **07**, 002, [arXiv:astro-ph/0603587](#).
- [82] R. Easther and H. Peiris, *JCAP* **09**, 010, [arXiv:astro-ph/0604214](#).
- [83] H. Peiris and R. Easther, *JCAP* **10**, 017, [arXiv:astro-ph/0609003](#).
- [84] K. I. Izawa, *Phys. Lett. B* **576**, 1 (2003), [arXiv:hep-ph/0305286](#).
- [85] A. Ashoorioon, J. L. Hovdebo, and R. B. Mann, *Nucl. Phys. B* **727**, 63 (2005), [arXiv:gr-qc/0504135](#).
- [86] G. Ballesteros, J. A. Casas, and J. R. Espinosa, *JCAP* **03**, 001, [arXiv:hep-ph/0601134](#).
- [87] M. Li, *JCAP* **10**, 003, [arXiv:astro-ph/0607525](#).
- [88] B. Chen, M. Li, T. Wang, and Y. Wang, *Mod. Phys. Lett. A* **22**, 1987 (2007), [arXiv:astro-ph/0610514](#).
- [89] V. Vennin, K. Koyama, and D. Wands, *JCAP* **11**, 008, [arXiv:1507.07575 \[astro-ph.CO\]](#).
- [90] A. Karam, T. Pappas, and K. Tamvakis, *Phys. Rev. D* **96**, 064036 (2017), [arXiv:1707.00984 \[gr-qc\]](#).
- [91] A. A. Starobinsky, *Sov. Astron. Lett.* **9**, 302 (1983).
- [92] A. A. Starobinsky and H. J. Schmidt, *Class. Quant. Grav.* **4**, 695 (1987).
- [93] A. Berera and L.-Z. Fang, *Phys. Rev. Lett.* **74**, 1912 (1995), [arXiv:astro-ph/9501024 \[astro-ph\]](#).
- [94] A. Berera, *Phys. Rev. Lett.* **75**, 3218 (1995), [arXiv:astro-ph/9509049 \[astro-ph\]](#).
- [95] A. Berera, I. G. Moss, and R. O. Ramos, *Rept. Prog. Phys.* **72**, 026901 (2009), [arXiv:0808.1855 \[hep-ph\]](#).
- [96] M. Bastero-Gil, A. Berera, R. O. Ramos, and J. G. Rosa, *JCAP* **01**, 016, [arXiv:1207.0445 \[hep-ph\]](#).

- [97] S. Bartrum, M. Bastero-Gil, A. Berera, R. Cerezo, R. O. Ramos, and J. G. Rosa, *Phys. Lett. B* **732**, 116 (2014), [arXiv:1307.5868 \[hep-ph\]](#).
- [98] S. Koh, B.-H. Lee, and G. Tumurtushaa, *Phys. Rev. D* **98**, 103511 (2018), [arXiv:1807.04424 \[astro-ph.CO\]](#).
- [99] J. de Haro, *Phys. Rev. D* **107**, 123511 (2023), [arXiv:2304.05903 \[gr-qc\]](#).
- [100] G. N. Felder, L. Kofman, and A. D. Linde, *Phys. Rev. D* **59**, 123523 (1999), [arXiv:hep-ph/9812289](#).
- [101] A. Shah, (2025), [arXiv:2510.22248 \[gr-qc\]](#).
- [102] M. J. P. Morse and W. H. Kinney, *Phys. Rev. D* **97**, 123519 (2018), [arXiv:1804.01927 \[astro-ph.CO\]](#).
- [103] S. D. Odintsov and V. K. Oikonomou, *Class. Quant. Grav.* **37**, 025003 (2020), [arXiv:1912.00475 \[gr-qc\]](#).
- [104] K. Dimopoulos, *Phys. Lett. B* **775**, 262 (2017), [arXiv:1707.05644 \[hep-ph\]](#).
- [105] E. D. Stewart and D. H. Lyth, *Phys. Lett. B* **302**, 171 (1993), [arXiv:gr-qc/9302019](#).
- [106] M. Drees and Y. Xu, *Phys. Lett. B* **867**, 139612 (2025), [arXiv:2504.20757 \[astro-ph.CO\]](#).
- [107] J. M. Maldacena, *JHEP* **0305**, 013, [arXiv:astro-ph/0210603 \[astro-ph\]](#).
- [108] D. Nandi and S. Shankaranarayanan, *JCAP* **06**, 038, [arXiv:1512.02539 \[gr-qc\]](#).
- [109] D. Nandi and S. Shankaranarayanan, *JCAP* **10**, 008, [arXiv:1606.05747 \[gr-qc\]](#).
- [110] D. Nandi, *Phys. Rev. D* **99**, 103532 (2019), [arXiv:1904.00153 \[gr-qc\]](#).
- [111] D. Nandi and L. Sriramkumar, *Phys. Rev. D* **101**, 043506 (2020), [arXiv:1904.13254 \[gr-qc\]](#).
- [112] D. Nandi, *Phys. Lett. B* **809**, 135695 (2020), [arXiv:2003.02066 \[astro-ph.CO\]](#).
- [113] D. Nandi, *Universe* **7**, 62 (2021), [arXiv:2009.03134 \[gr-qc\]](#).
- [114] D. Nandi and M. Kaur, (2022), [arXiv:2206.08335 \[astro-ph.CO\]](#).
- [115] D. Nandi and M. Kaur, *Phys. Dark Univ.* **44**, 101430 (2024), [arXiv:2302.03413 \[astro-ph.CO\]](#).
- [116] M. Kaur, D. Nandi, D. Choudhury, and T. R. Seshadri, *Int. J. Mod. Phys. D* **33**, 2450006 (2024), [arXiv:2302.13698 \[astro-ph.CO\]](#).